

Influence of polarization on the optical chirality of vortex beams

Dale Green and Kayn A. Forbes*

School of Chemistry, University of East Anglia, Norwich NR4 7TJ, United Kingdom

*k.forbes@uea.ac.uk

ABSTRACT

It is well understood that circularly polarized light possesses optical chirality. This optical chirality can engage with material chirality, leading to optical activity, the underlying physics of chiroptical spectroscopy. Optical vortex beams with azimuthal phase possess helical wavefronts that are chiral. Under spatial confinement (e.g. tight focusing), the polarization state of the input beam and the geometrical wavefront chirality are not independent of one another, and their interplay significantly influences the optical chirality density of the beam. Here we highlight how the state of input beam polarization, e.g. linear, elliptical, and circular, influences the optical chirality of vortex beams. We show that the spatial distributions of the optical chirality density are acutely dependent on the polarization of the input beam, alongside other characteristics like the topological charge and radial index. Most striking is that even an unpolarized optical vortex beam possesses non-zero optical chirality density.

Keywords: Optical chirality, optical helicity, chirality, structured light, optical activity, optical vortex, non-paraxial, nano optics

1. INTRODUCTION

Chirality is pervasive in life: essentially all biomolecules and drugs are chiral, their biological functions acutely linked to their handedness. Beyond material chirality, light may also be chiral. The most famous example of chiral light is that which is circularly polarized: the electromagnetic field vectors trace out a helical structure on propagation. One of the most prominent methods to study material chirality is using chiral light, in a range of techniques known collectively as chiroptical spectroscopy¹⁻³. Beyond the chirality associated with circularly polarization, light can also possess a chiral structure if it possesses an azimuthal phase $\exp(i\ell\phi)$, where $\ell \in \mathbb{Z}$ is known as the topological charge. This azimuthal phase leads to helical wavefronts (surfaces of constant phase), the sign of ℓ determines whether the wavefront twists to the left or the right. Of course, it is this azimuthal phase structured which is responsible for the optical orbital angular momentum (OAM) of optical vortex beams, such as Laguerre-Gaussian and Bessel modes. Applications of optical vortex beams have been widespread but utilizing its wavefront chirality has only recently seen research activity, in particular since 2018. The reader is referred to reference⁴ for a recent topical review.

The most recent and exciting developments include experiments exploiting this vortex chirality include x-ray vortex dichroism in chiral organometallic complexes⁵, vortex Raman optical activity of chiral molecular fluids^{6,7}; and nonlinear vortex dichroism in chiral molecules as small as limonene and fenchone⁸. Another remarkable result recently discovered is that an optical vortex possesses a non-zero optical chirality even if the input beam is unpolarized^{9,10}, that is, chiral light-matter interactions can be achieved with unpolarized light. Building on this result, in this work we study how the optical chirality density of tightly-focused Laguerre-Gauss and Bessel vortex beams are influenced by the input state of polarization.

2. LAGUERRE-GAUSSIAN MODE

The cycle-averaged optical chirality density \bar{C} for monochromatic fields is given by the formula^{11,12}

$$\bar{C} = -\frac{\omega\epsilon_0}{2}\text{Im}[\mathbf{E}^* \cdot \mathbf{B}], \quad (1)$$

where ω is the angular frequency of the optical field and $*$ denotes the complex conjugate. By inserting the appropriate electric \mathbf{E} and magnetic fields \mathbf{B} , the optical chirality density (1) gives some idea of how chiral the electromagnetic field is. For a plane wave, the optical chirality is zero for linearly polarized or unpolarized light; it is non-zero for elliptically polarized light, and maximum for circularly polarized light $\bar{C} = \sigma I \omega c^{-2}$, $\sigma = \pm 1$ is the helicity (upper sign denotes left-handed light; lower sign right-handed light). The chirality of optical vortex beams, such as Laguerre-Gaussian and Bessel, have seen a recent surge in interest due to the fact they possess non-zero optical chirality (1) even when they possess no degree of ellipticity, i.e. they are linearly polarized or unpolarized. For more details the reader is referred to references^{9,13,14}. It is crucial to point out that when we speak of polarization in this work, we explicitly mean the two-dimensional (2D) polarization state, i.e., that of the paraxial transverse electromagnetic fields in the far field, and not that of the polarization of the field around the focal plane, which is described by the three-dimensional (3D) state of polarization due to the generation of significant longitudinal electromagnetic fields.¹⁵⁻¹⁷

The optical chirality density for a Laguerre-Gaussian beam, including the longitudinal fields generated by tight-focusing, is given by¹⁴

$$\begin{aligned} \bar{C}_{\text{LG}} = & -\frac{I_{\text{LG}}(r, z)\omega}{c^2}\text{Im}\left[(\alpha\beta^* - \alpha^*\beta) \right. \\ & \left. + \frac{1}{k^2}\left(\left\{|\alpha|^2 + |\beta|^2\right\}\frac{i\ell}{r}\gamma + \alpha\beta^*\left\{|\gamma|^2\sin^2\phi + \frac{\ell^2}{r^2}\cos^2\phi\right\} - \alpha^*\beta\left\{|\gamma|^2\cos^2\phi + \frac{\ell^2}{r^2}\sin^2\phi\right\}\right)\right]. \end{aligned} \quad (2)$$

$I_{\text{LG}}(r, z)$ is the intensity of the Laguerre-Gaussian mode; ω is the angular frequency; α is the x -component and β the y -component of the corresponding Jones vector for a given polarisation state; k is the wave number; ℓ is the topological charge; r is the radial coordinate; and

$$\gamma = \left[\frac{|\ell|}{r} - \frac{2r}{w^2} + \frac{ikr}{R} - \frac{4r}{w^2} \frac{L_p^{|\ell|+1}}{L_p^{|\ell|}} \right], \quad (3)$$

where R is the wavefront curvature; w is the beam waist; and $L_p^{|\ell|}$ is the Laguerre polynomial with p the radial index. By varying the values of α and β we can study the influence the input (2D) polarization state of the beam has upon the optical chirality density of the field in the focal plane.

For the most general Jones vector $\alpha = \cos \eta \cos \theta - i \sin \eta \sin \theta$ and $\beta = -\cos \eta \sin \theta - i \sin \eta \cos \theta$, where θ is the azimuth of the polarization ellipse, and η is the ellipticity. Inserting these into (2) gives

$$\bar{C}_{\text{LG}} = -\frac{I_{\text{LG}}(r, z)\omega}{c^2} \left[\sin 2\eta + \frac{\text{Re}}{k^2} \left(\frac{\ell}{r} \gamma + \frac{\sin 2\eta}{2} \left\{ |\gamma|^2 + \frac{\ell^2}{r^2} \right\} \right) \right]. \quad (4)$$

A positive (negative) ellipticity in (4) corresponds to right-handed (left-handed) polarization; $\eta = \pm\pi/4$ corresponds to circularly polarised light; $\eta = 0$ corresponds to linear polarization; averaging (4) over two orthogonal polarizations gives the unpolarized result, e.g. $\eta = \pi/4$ and $\eta = -\pi/4$. Furthermore, (4) does not depend on θ which is the azimuth. The first term in square brackets of (4) is the generally dominant contribution to the optical chirality density, proportional to the degree of ellipticity. It is this dominant term, which is the contribution present in paraxial, well-collimated laser beams, directly analogous to the optical chirality density of a plane wave. The second term in square brackets stems purely from the longitudinal fields, generated by tight focusing, and has no plane wave equivalent due to the strict absence of longitudinal fields in plane waves. To see how the optical chirality density in the focal plane $z = 0$ varies with changing the input beam 2D polarization we have plotted (4) for varying degrees of ellipticity η in Figures 1-8.

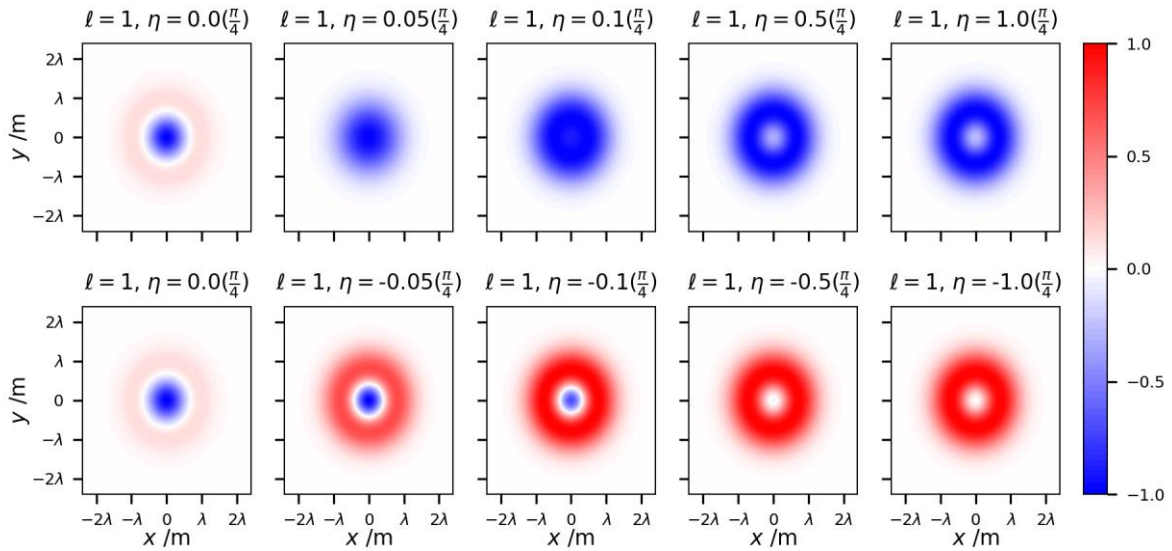


Figure 1: Evolution of the optical chirality density of an $\ell = 1, p = 0$ Laguerre-Gaussian beam in the focal plane with varying 2D-polarization ellipticity η . The input polarization progresses from linearly polarized $\eta = 0$ through varying degrees of ellipticity $-\pi/4 < \eta < \pi/4$ until it reaches pure circular polarisation $\eta = \pm\pi/4$. The top row cycles through right-handed polarization; the bottom row left-handed polarization. In all plots $w_0 = \lambda$.

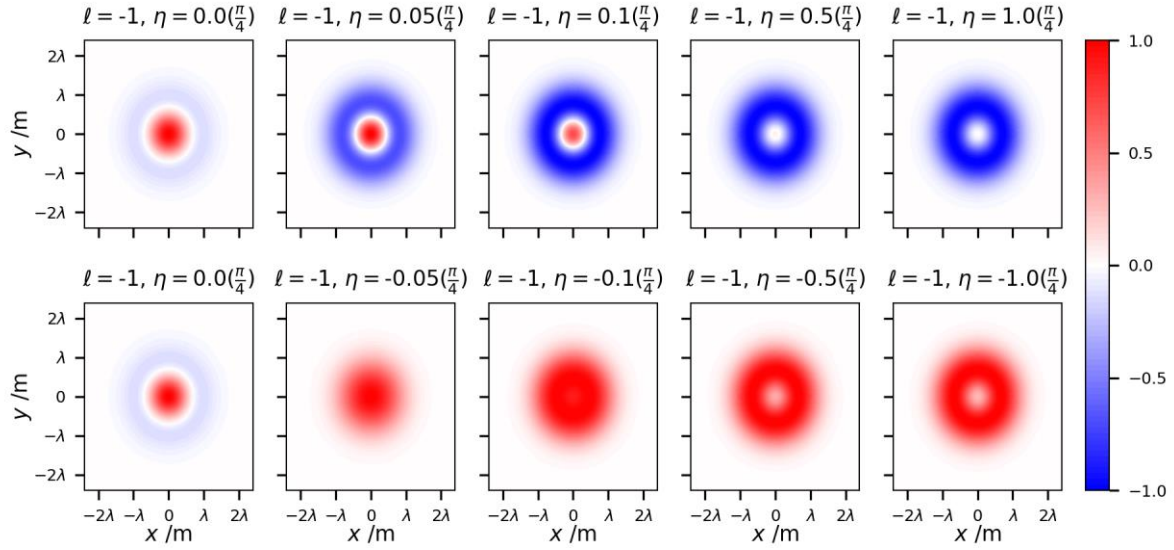


Figure 2: Evolution of the optical chirality density of an $\ell = -1, p = 0$ Laguerre-Gaussian beam in the focal plane with varying 2D-polarization ellipticity η . The input polarization progresses from linearly polarized $\eta = 0$ through varying degrees of ellipticity $-\pi/4 < \eta < \pi/4$ until it reaches pure circularly polarisation $\eta = \pm\pi/4$. The top row cycles through right-handed polarization; the bottom row left-handed polarization. In all plots $w_0 = \lambda$.

The figures highlight several interest effects of the optical chirality density of vortex beams and how it depends on the 2D polarization of the input beam. For example:

- 1) There is a 2D polarization-independent optical chirality density generated by linearly polarized and unpolarized optical vortices, even though they possess $\eta = 0$ in the far field.
- 2) The sign of this optical chirality density (when $\eta = 0$) is determined solely by $\text{sgn } \ell$. This allows for chiral light-matter interactions that are not dependent on the 2D polarization handedness¹⁸.
- 3) When the vortex handedness $\text{sgn } \ell$ is opposite to the polarization handedness $\text{sgn } \eta$ we produce on-axis chirality densities for $|\ell| = 1$ and a tighter focal spot in general. This is well known behaviour for the energy density of non-paraxial beams. When the vortex handedness $\text{sgn } \ell$ is the same as the polarization handedness $\text{sgn } \eta$ there is always a null of chirality density at some point.
- 4) When $\eta \neq 0$ the handedness of the polarization has a much more significant influence on the sign of optical chirality than the vortex handedness.
- 5) For small degrees of ellipticity the optical chirality density produces the spatial distribution of a Gaussian spot (increasing the ellipticity leads to the rapid formation of a doughnut shape). #

The effects of increasing ℓ and p are given in Figures 3-8.

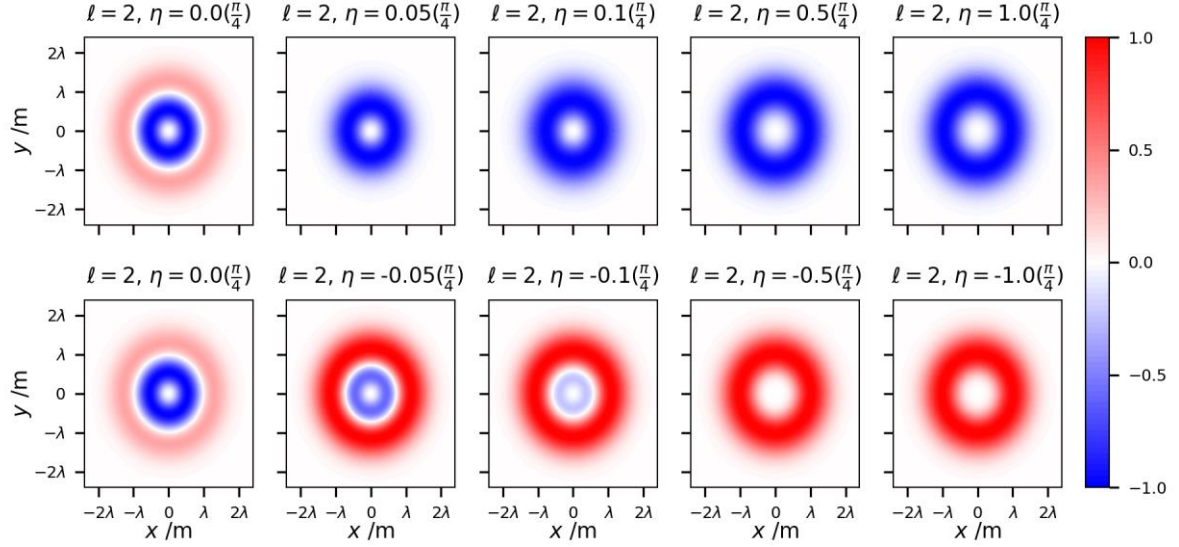


Figure 3: Evolution of the optical chirality density of an $\ell = 2, p = 0$ Laguerre-Gaussian beam in the focal plane with varying 2D-polarization ellipticity η . The input polarization progresses from linearly polarized $\eta = 0$ through varying degrees of ellipticity $-\pi/4 < \eta < \pi/4$ until it reaches pure circularly polarisation $\eta = \pm\pi/4$. The top row cycles through right-handed polarization; the bottom row left-handed polarization. In all plots $w_0 = \lambda$.

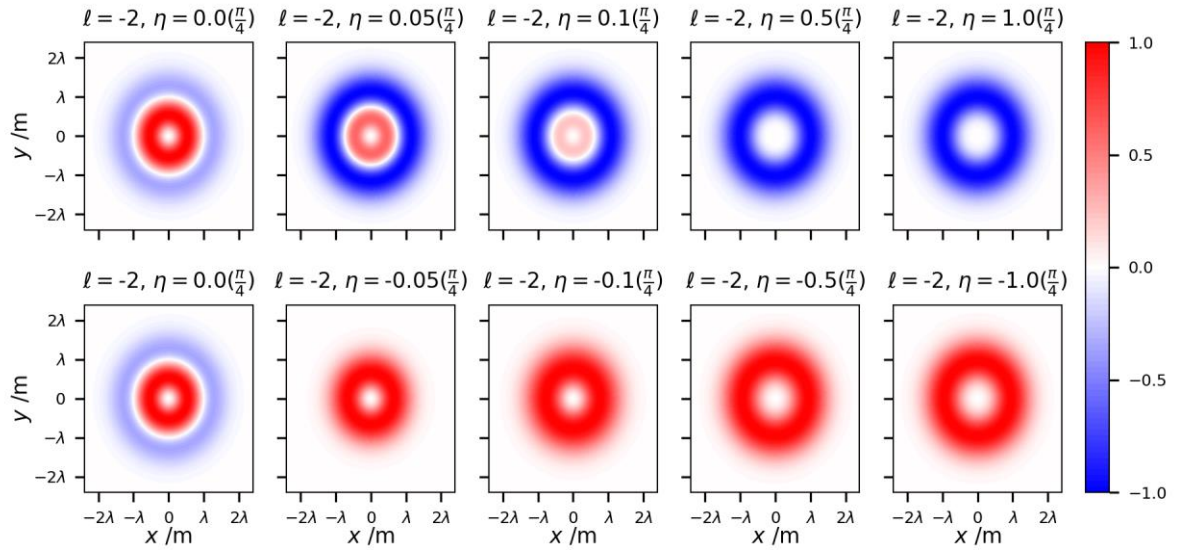


Figure 4: Evolution of the optical chirality density of an $\ell = -2, p = 0$ Laguerre-Gaussian beam in the focal plane with varying 2D-polarization ellipticity η . The input polarization progresses from linearly polarized $\eta = 0$ through varying degrees of ellipticity $-\pi/4 < \eta < \pi/4$ until it reaches pure circularly polarisation $\eta = \pm\pi/4$. The top row cycles through right-handed polarization; the bottom row left-handed polarization. In all plots $w_0 = \lambda$.

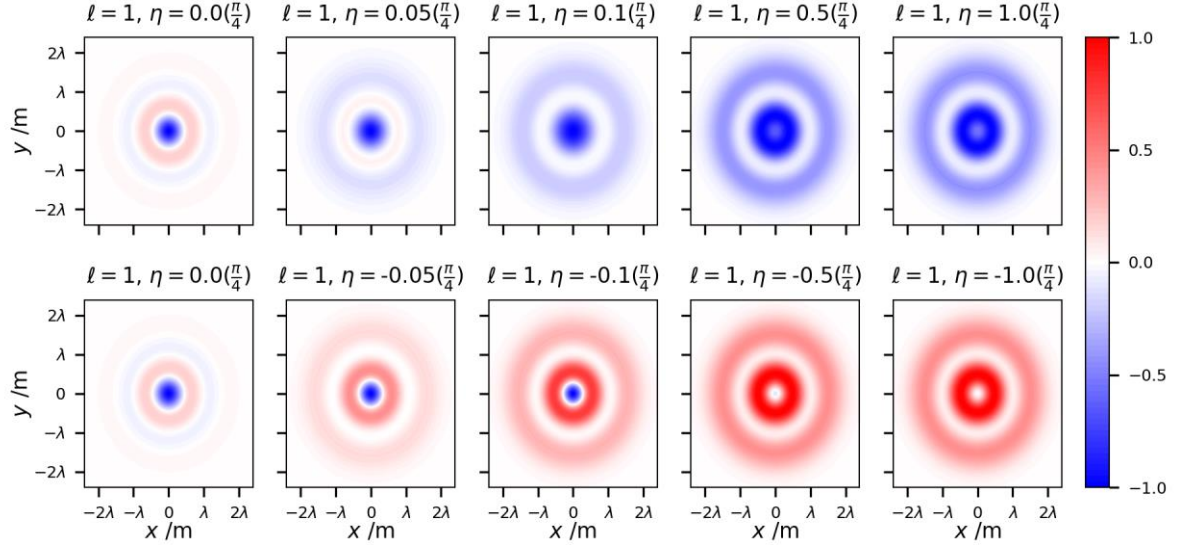


Figure 5: Evolution of the optical chirality density of an $\ell = 1, p = 1$ Laguerre-Gaussian beam in the focal plane with varying 2D-polarization ellipticity η . The input polarization progresses from linearly polarized $\eta = 0$ through varying degrees of ellipticity $-\pi/4 < \eta < \pi/4$ until it reaches pure circularly polarisation $\eta = \pm\pi/4$. The top row cycles through right-handed polarization; the bottom row left-handed polarization. In all plots $w_0 = \lambda$.

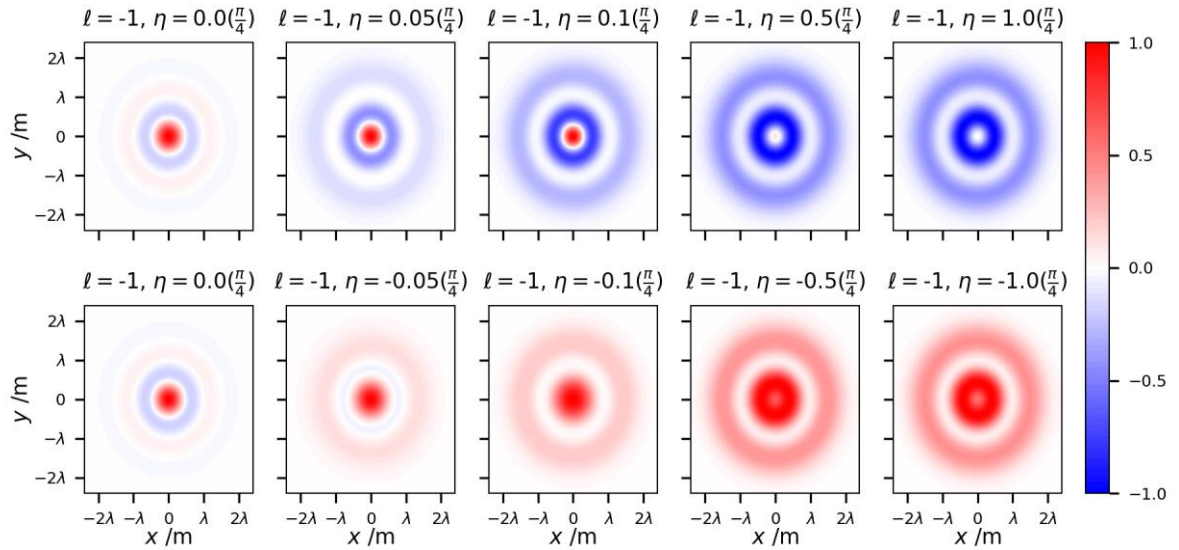


Figure 6: Evolution of the optical chirality density of an $\ell = -1, p = 1$ Laguerre-Gaussian beam in the focal plane with varying 2D-polarization ellipticity η . The input polarization progresses from linearly polarized $\eta = 0$ through varying degrees of ellipticity $-\pi/4 < \eta < \pi/4$ until it reaches pure circularly polarisation $\eta = \pm\pi/4$. The top row cycles through right-handed polarization; the bottom row left-handed polarization. In all plots $w_0 = \lambda$.

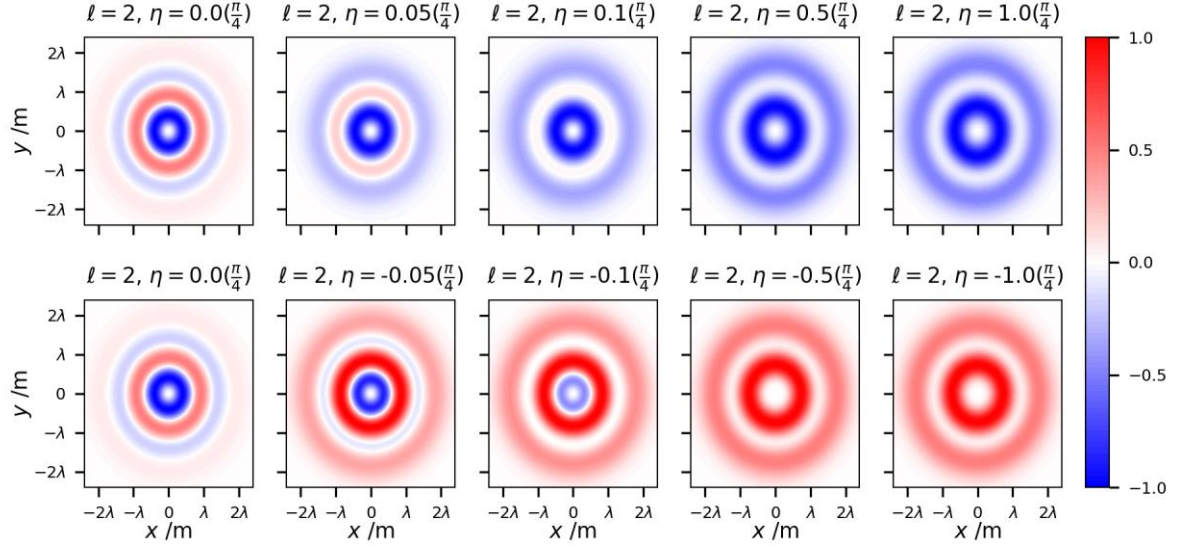


Figure 7: Evolution of the optical chirality density of an $\ell = 2, p = 1$ Laguerre-Gaussian beam in the focal plane with varying 2D-polarization ellipticity η . The input polarization progresses from linearly polarized $\eta = 0$ through varying degrees of ellipticity $-\pi/4 < \eta < \pi/4$ until it reaches pure circularly polarisation $\eta = \pm\pi/4$. The top row cycles through right-handed polarization; the bottom row left-handed polarization. In all plots $w_0 = \lambda$.

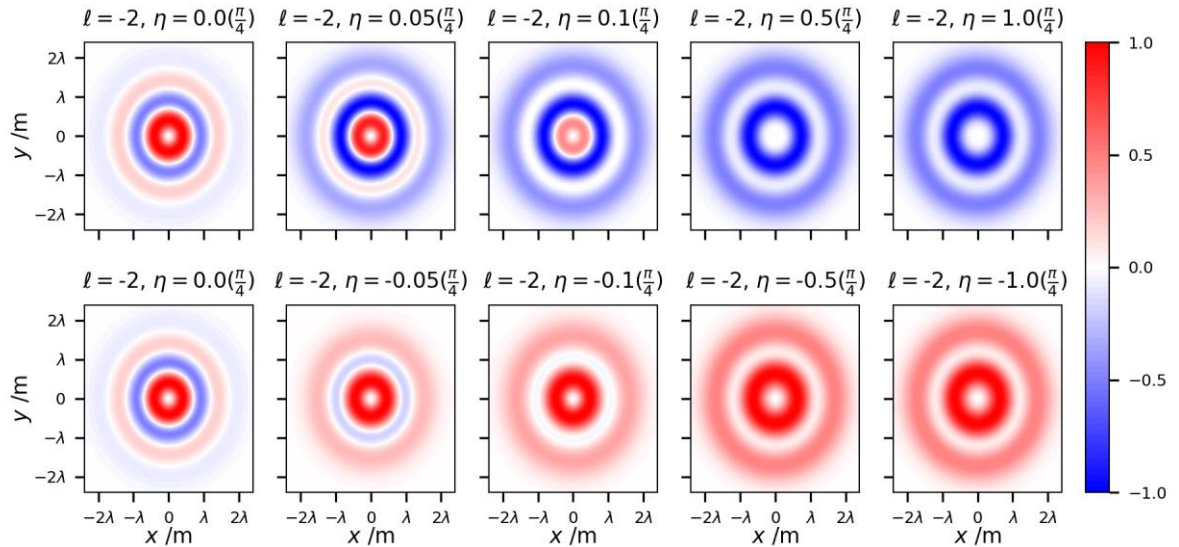


Figure 8: Evolution of the optical chirality density of an $\ell = -2, p = 1$ Laguerre-Gaussian beam in the focal plane with varying 2D-polarization ellipticity η . The input polarization progresses from linearly polarized $\eta = 0$ through varying degrees of ellipticity $-\pi/4 < \eta < \pi/4$ until it reaches pure circularly polarisation $\eta = \pm\pi/4$. The top row cycles through right-handed polarization; the bottom row left-handed polarization. In all plots $w_0 = \lambda$.

3. BESSEL MODE

The optical chirality density for a Bessel beam is given by¹⁴

$$\bar{C}_B = -\frac{I\omega}{c^2} \text{Im} \left[\frac{k_z}{k} (\alpha\beta^* - \alpha^*\beta) J_\ell^2 + \left(\frac{k_r^2}{4kk_z} \right) \left(\{-i\beta^* + \alpha^*\} \{i\alpha - \beta\} J_{\ell-1}^2 + \{i\alpha + \beta\} \{-i\beta^* - \alpha^*\} J_{\ell+1}^2 \right) \right]. \quad (5)$$

Once again, by utilizing the most general Jones vector components we produce the following form of the optical chirality density of a Bessel beam

$$\bar{C}_B = -\frac{I\omega}{c^2} \left[\frac{k_z}{k} J_\ell^2 \sin 2\eta + \left(\frac{k_r^2}{4kk_z} \right) \left(\{\sin 2\eta + 1\} J_{\ell-1}^2 + \{\sin 2\eta - 1\} J_{\ell+1}^2 \right) \right]. \quad (6)$$

The optical chirality densities (6) are plotted in Figures 9-12 for $z = 0$. The characteristics of the optical chirality density in the focal plane for a Bessel mode are like that of the LG mode, apart from the obvious fact that Bessel modes have many more concentric rings, appearing like a high- p valued LG beam.

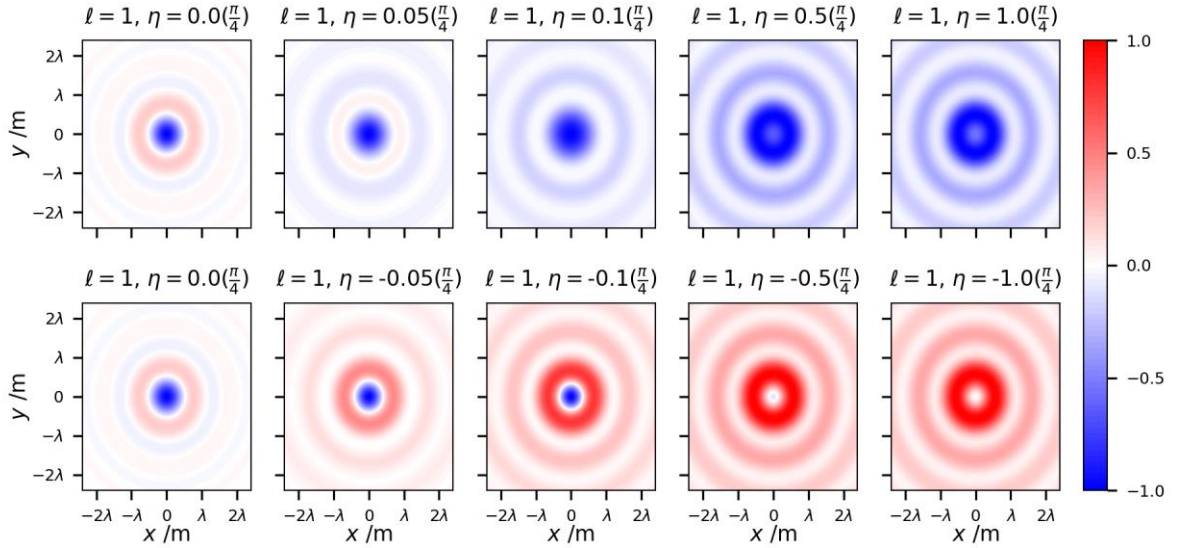


Figure 9: Evolution of the optical chirality density of an $\ell = 1$ Bessel beam in the focal plane with varying 2D-polarization ellipticity η . The input polarization progresses from linearly polarized $\eta = 0$ through varying degrees of ellipticity $-\pi/4 < \eta < \pi/4$ until it reaches pure circularly polarisation $\eta = \pm\pi/4$. The top row cycles through right-handed polarization; the bottom row left-handed polarization. In all plots $k_r/k_z = 0.63$ which makes the plots comparable to the LG beams in Section 2 in terms of spatial confinement of the field.

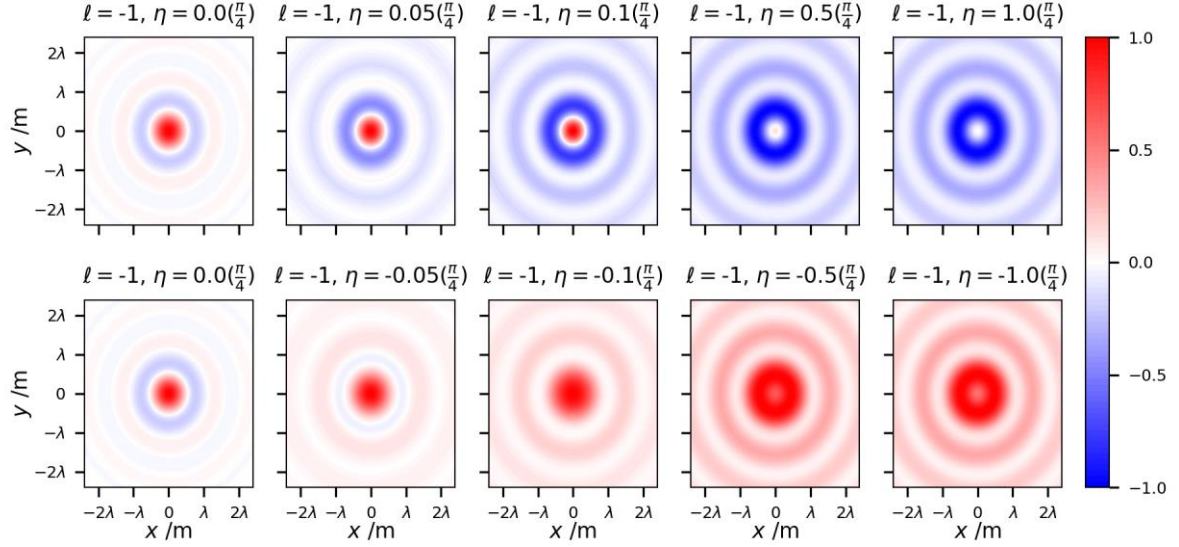


Figure 10: Evolution of the optical chirality density of an $\ell = -1$ Bessel beam in the focal plane with varying 2D-polarization ellipticity η . The input polarization progresses from linearly polarized $\eta = 0$ through varying degrees of ellipticity $-\pi/4 < \eta < \pi/4$ until it reaches pure circularly polarisation $\eta = \pm\pi/4$. The top row cycles through right-handed polarization; the bottom row left-handed polarization. In all plots $k_r/k_z = 0.63$ which makes the plots comparable

to the LG beams in Section 2 in terms of spatial confinement of the field.

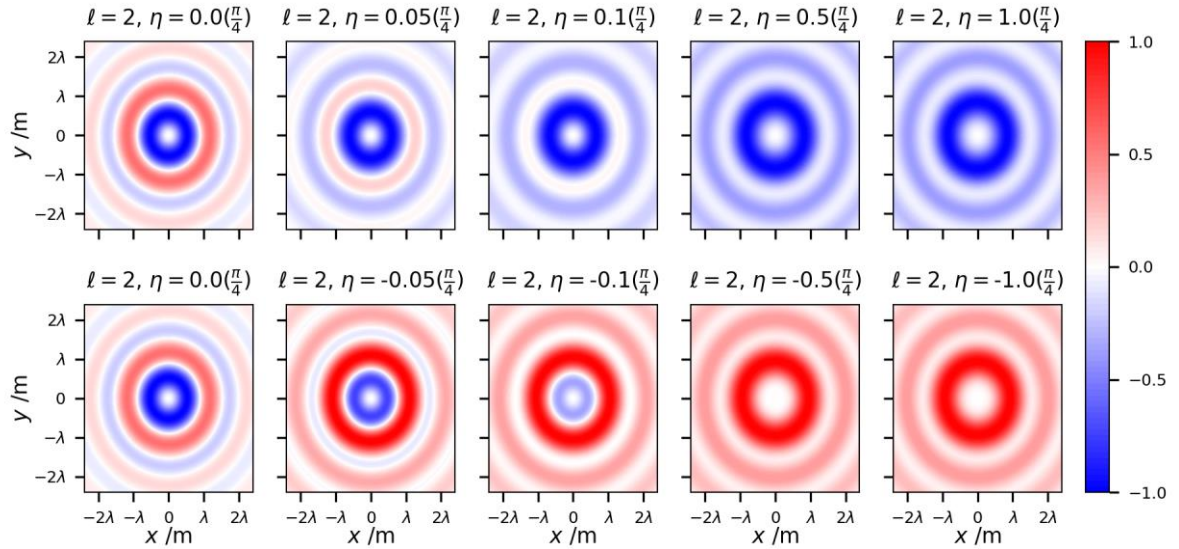


Figure 11: Evolution of the optical chirality density of an $\ell = 2$ Bessel beam in the focal plane with varying 2D-polarization ellipticity η . The input polarization progresses from linearly polarized $\eta = 0$ through varying degrees of ellipticity $-\pi/4 < \eta < \pi/4$ until it reaches pure circularly polarisation $\eta = \pm\pi/4$. The top row cycles through right-handed polarization; the bottom row left-handed polarization. In all plots $k_r/k_z = 0.63$ which makes the plots comparable

to the LG beams in Section 2 in terms of spatial confinement of the field.

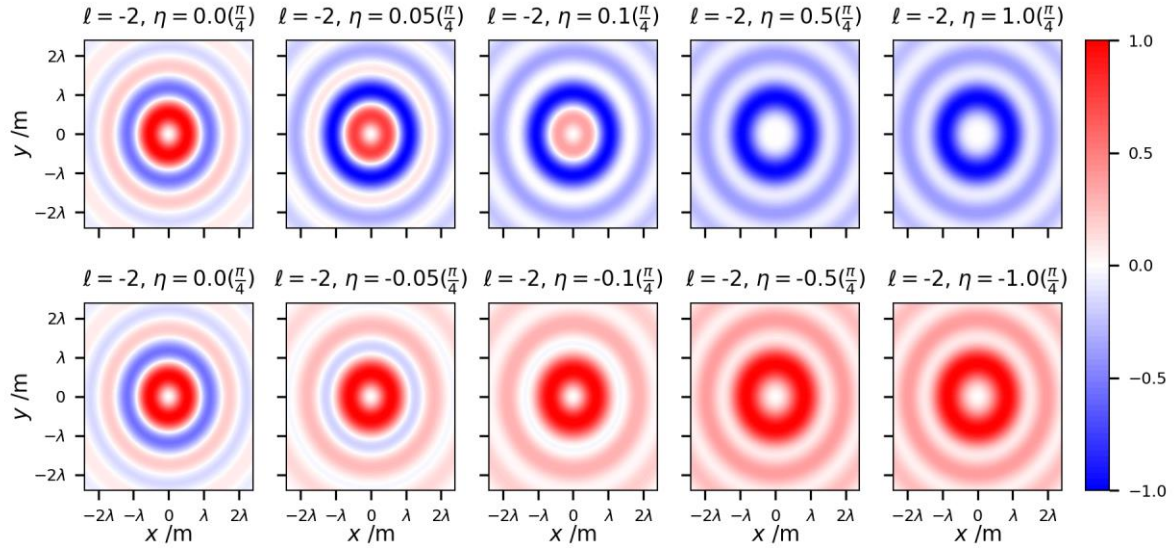


Figure 12: Evolution of the optical chirality density of an $\ell = -2$ Bessel beam in the focal plane with varying 2D-polarization ellipticity η . The input polarization progresses from linearly polarized $\eta = 0$ through varying degrees of ellipticity $-\pi/4 < \eta < \pi/4$ until it reaches pure circularly polarisation $\eta = \pm\pi/4$. The top row cycles through right-handed polarization; the bottom row left-handed polarization. In all plots $k_t/k_z = 0.63$ which makes the plots comparable

to the LG beams in Section 2 in terms of spatial confinement of the field.

5. CONCLUSION

In this work we have highlighted how the optical chirality density of vortex beams is influenced by the state of 2D polarization. Optical vortex beams are unique electromagnetic fields that possess optical chirality even when linearly polarized, or even unpolarized, in a 2D sense. Going from a linearly polarized beam and increasing the ellipticity of the input field drastically alters the optical chirality in the focal plane. Furthermore, the polarisation handedness and wavefront handedness also play a significant role in the spatial distribution of optical chirality in the focal plane.

REFERENCES

1. Polavarapu, P. L. *Chiral Analysis: Advances in Spectroscopy, Chromatography and Emerging Methods*. (Elsevier Science, 2018).
2. Berova, N., Polavarapu, P. L., Nakanishi, K. & Woody, R. W. *Comprehensive Chiroptical Spectroscopy: Instrumentation, Methodologies, and Theoretical Simulations*. vol. 1 (John Wiley & Sons, 2011).
3. Berova, N., Polavarapu, P. L., Nakanishi, K. & Woody, R. W. *Comprehensive chiroptical spectroscopy: applications in stereochemical analysis of synthetic compounds, natural products, and biomolecules*. vol. 2 (John Wiley & Sons, 2012).

4. Forbes, K. A. & Andrews, D. L. Orbital angular momentum of twisted light: chirality and optical activity. *J. Phys. Photonics* **3**, 022007 (2021).
5. Rouxel, J. R. *et al.* Hard X-ray helical dichroism of disordered molecular media. *Nat. Photonics* **16**, 570–574 (2022).
6. Büscher, F. *et al.* Raman scattering of plane-wave and twisted light off chiral molecular liquids. *Low Temp. Phys.* **47**, 959–965 (2021).
7. Müllner, S., Büscher, F., Möller, A. & Lemmens, P. Discrimination of Chiral and Helical Contributions to Raman Scattering of Liquid Crystals Using Vortex Beams. *Phys. Rev. Lett.* **129**, 207801 (2022).
8. Bégin, J.-L. *et al.* Nonlinear helical dichroism in chiral and achiral molecules. *Nat. Photonics* **17**, 82–88 (2023).
9. Forbes, K. A. Optical helicity of unpolarized light. *Phys. Rev. A* **105**, 023524 (2022).
10. Forbes, K. A. & Green, D. Enantioselective optical gradient forces using 3D structured vortex light. *Opt. Commun.* **515**, 128197 (2022).
11. Tang, Y. & Cohen, A. E. Optical chirality and its interaction with matter. *Phys. Rev. Lett.* **104**, 163901 (2010).
12. Cameron, R. P., Barnett, S. M. & Yao, A. M. Optical helicity, optical spin and related quantities in electromagnetic theory. *New J. Phys.* **14**, 053050 (2012).
13. Forbes, K. A. & Jones, G. A. Measures of helicity and chirality of optical vortex beams. *J. Opt.* **23**, 115401 (2021).
14. Green, D. & Forbes, K. A. Optical chirality of vortex beams at the nanoscale. *Nanoscale* **15**, 540–552 (2023).
15. Alonso, M. A. Geometric descriptions for the polarization for nonparaxial optical fields: a tutorial. *ArXiv Prepr. ArXiv200802720* (2020).
16. Lindfors, K., Setälä, T., Kaivola, M. & Friberg, A. T. Degree of polarization in tightly focused optical fields. *JOSA A* **22**, 561–568 (2005).
17. Setälä, T., Shevchenko, A., Kaivola, M. & Friberg, A. T. Degree of polarization for optical near fields. *Phys. Rev. E* **66**, 016615 (2002).
18. Forbes, K. A. & Jones, G. A. Optical vortex dichroism in chiral particles. *Phys. Rev. A* **103**, 053515 (2021).